THE JOURNAL OF BIOLOGICAL CHEMISTRY
Vol. 271, No. 30, Issue of July 26, pp. 17903–17910, 1996

Printed in U.S.A.

Molecular Cloning and Functional Expression of Mouse Connexin-30, a Gap Junction Gene Highly Expressed in Adult Brain and Skin*

(Received for publication, March 4, 1996, and in revised form, May 9, 1996)

Edgar Dahl‡§, Dieter Manthey‡, Ye Chen¶, Hans-Jürgen Schwarz‡, Young Sook Chang‖, Peter A. Lalley‖, Bruce J. Nicholson¶, and Klaus Willecke‡**

From the ‡Institut für Genetik, Abteilung Molekulargenetik, Universität Bonn, 53117 Bonn, Federal Republic of Germany, the §GSF Forschungszentrum für Umwelt und Gesundheit, 85764 Oberschleißheim, Federal Republic of Germany, the ¶Department of Biological Sciences, State University of New York, Buffalo, New York 14260, and the ‖Rochester Institute of Technology, National Technical Institute for the Deaf, Rochester, New York 14623-5604

A new gap junction gene isolated from the mouse genome codes for a connexin protein of 261 amino acids. Because of its theoretical molecular mass of 30.366 kDa, it is named connexin-30. Within the connexin gene family, this protein is most closely related to connexin-26 (77% amino acid sequence identity). The coding region of mouse connexin-30 is uninterrupted by introns and is detected in the mouse genome as a single copy gene that is assigned to mouse chromosome 14 by analysis of mouse × hamster somatic cell hybrids. Abundant amounts of connexin-30 mRNA (two transcripts of 2.0 and 2.3 kilobase pairs) were found after 4 weeks of postnatal development in mouse brain and skin. Microinjection of connexin-30 cRNA into *Xenopus* oocytes induced formation of functional gap junction channels that gated somewhat asymmetrically in response to transjunctional voltage and at significantly lower voltage (V_o = +38 and −46 mV) than the closely homologous connexin-26 channels (V_o = 89 mV). Heterotypic pairings of connexin-30 with connexin-26 and connexin-32 produced channels with highly asymmetric and rectifying voltage gating, respectively. This suggests that the polarity of voltage gating and the cationic selectivity of connexin-30 are similar to those of its closest homologue, connexin-26.

The connexin gene family codes for the protein subunits of gap junction channels that mediate direct diffusion of ions and metabolites between the cytoplasm of adjacent cells (reviewed by Bennett *et al.* (1991), Beyer (1993), Paul (1995), and White *et al.* (1995)). Functional gap junctions have been suggested to be involved in metabolic cooperation between cells, synchronization of cellular physiological activities, growth control, and regulation of development.

To date, 12 different connexin genes have been characterized in the mouse or rat genome (Willecke *et al.*, 1991a; Haefliger *et al.*, 1992; White *et al.*, 1992) and assigned to different chromosomal localizations (Haefliger *et al.*, 1992; Schwarz *et al.*, 1992, 1994). Connexin genes are expressed in a cell type-specific manner with overlapping specificity. Based on analyses of amino acid sequences and labeling of membrane-embedded connexins with peptide-specific antibodies (Milks *et al.*, 1988; Yancey *et al.*, 1989; Zhang and Nicholson, 1994), a general topology of connexin proteins was proposed. It was deduced that the polypeptide chain of connexins spans the plasma membrane four times, with amino- and carboxyl-terminal regions facing the cytoplasm. By comparison within the gene family, connexins show very high sequence identities in the transmembrane regions and in the two extracellular loops, which are presumably responsible for the docking of two hemichannels. Major differences have been found in the central cytoplasmic loop and carboxyl-terminal tail in terms of length as well as sequence. Cloned connexin (Cx)[1] genes have been functionally expressed in *Xenopus* oocytes and cultured mammalian cells (reviewed by Paul (1995) and White *et al.* (1995)). These reconstitution experiments have shown that gap junction channels have unique properties depending on the type of connexin(s) constituting the channel.

Reconstitution of connexin channels in cultured mammalian cells has revealed that channel conductance can depend on phosphorylation of the Cx43 protein (Moreno *et al.*, 1994) and that connexin channels exhibit different permeabilities to tracer molecules (Elfgang *et al.*, 1995). Furthermore, connexins show specificity in terms of the functional docking of their hemichannels. Some combinations are compatible (*e.g.* Cx26 and Cx32 (Barrio *et al.*, 1991) as well as Cx40 and Cx37 (Hennemann *et al.*, 1992a)), while others (Cx40 and Cx43) do not form functional gap junctions in *Xenopus* oocytes (Bruzzone *et al.*, 1993) or cultured mammalian cells (Elfgang *et al.*, 1995).

To understand all aspects of gap junctional communication between different mammalian cells, it is necessary to characterize all functional connexin channels and their protein constituents. In this paper, we describe the characterization of Cx30, a new member of the murine connexin gene family, which is highly expressed in adult skin and brain, but is not detected in embryonic and fetal brain. This expression pattern is clearly different from that of the closely related Cx26 gene. When expressed in *Xenopus* oocytes, Cx30 and Cx26 channels show the same voltage gating polarity. However, the specific parameters, describing the voltage sensitivity of these channels, vary between Cx30 and Cx26. This system of two highly sequence-related connexin proteins can be used to search for the molecular basis of the differences in channel gating and other parameters.

MATERIALS AND METHODS

Isolation of Genomic Mouse Cx30 DNA—Previously, we isolated 25 connexin homologous recombinant EMBL3 phage clones by screening of

* This work was supported by Deutsche Forschungsgemeinschaft Grant SFB 284 (Project C1) and a grant from the Fonds der Chemischen Industrie (to K. W.), National Institutes of Health Grants CA-48049 and HL-48773 (to B. J. N.), and a common Max Planck research prize (to B. J. N. and K. W.). The costs of publication of this article were defrayed in part by the payment of page charges. This article must therefore be hereby marked "*advertisement*" in accordance with 18 U.S.C. Section 1734 solely to indicate this fact.

** To whom correspondence should be addressed: Institut für Genetik, Abt. Molekulargenetik, Römerstr. 164, 53117 Bonn, FRG. Tel.: 228-550-211; Fax: 228-550-263.

[1] The abbreviations used are: Cx, connexin; kb, kilobase pair(s).

a genomic C57/Bl6 mouse library with a rat Cx26 probe (Willecke *et al.*, 1991b). The procedure used to determine which connexin genes were represented among the recombinant phages is described by Hennemann *et al.* (1992a). Several phage clones were identified that did not hybridize to any of the known connexin genes under stringent conditions (50% formamide, 5 × SSC at 42 °C). DNA of one of these latter phages was isolated using standard protocols (Sambrook *et al.*, 1989). Southern blot hybridization of restricted phage DNA was performed under reduced stringency (40% formamide, 5 ×SSC at 37 °C) using the rat Cx32 cDNA probe (Paul, 1986). It was concluded that two adjacent fragments (0.5-kb *Kpn*I and 3.5-kb *Kpn*I/*Sac*I) contained sequences homologous to the Cx32 gene probe. These fragments, in addition to the complete insert of the recombinant phage (10.5 kb), were subcloned in pBluescript SK$^+$ (Stratagene, La Jolla, CA). Sequencing was performed on both strands by the modified chain termination method (Tabor and Richardson, 1987) using either vector-derived primers or appropriate primers derived from previous sequencing results. The amino acid sequence deduced from the longest open reading frame (*i.e.* mouse Cx30) was aligned with different connexin sequences using the Microgenie sequence analysis program (Beckman Instruments).

Southern and Northern Blot Analyses—Genomic DNA from livers of BALB/c mice was prepared according to a standard procedure (Sambrook *et al.*, 1989). Restriction endonuclease-digested DNA (10 μg) was electrophoresed in 0.7% agarose and blotted by alkaline transfer onto Hybond N membrane following the manufacturer's directions (Amersham International, Buckinghamshire, United Kingdom). High stringency hybridization of the Southern blot was carried out overnight using two different polymerase chain reaction fragments of ~600 base pairs amplified from the cloned mouse Cx30 gene. These fragments (representing nucleotides 25–615 and 203–760 in Fig. 2, respectively) were labeled with [α-^{32}P]dCTP by random priming (Amersham Buchler, Braunschweig, Germany) to a specific activity of 0.2–1 × 10^9 cpm/μg of DNA. Filters were washed at high stringency (0.2 × SSC, 0.1% SDS at 60 °C) and exposed to Kodak XAR-5 film for 5 days. Identical hybridization signals were obtained with both labeled DNA probes.

Total RNA from mouse tissues was isolated, electrophoresed, and blotted as described previously (Hennemann *et al.*, 1992a). Northern blot hybridization with the Cx30 probe was carried out under the same conditions as described above for Southern blot hybridization. Specific mRNA signals on autoradiographs were quantified by densitometric evaluation using Scan Pack Version 14.1A27 (Biometra, Göttingen, Germany).

Determination of Poly(A)$^+$ mRNA Abundance—The amount of poly(A)$^+$ RNA in different samples was compared by hybridization to oligo(dT) as described by Harley (1987) with slight modifications. Total cellular RNA was quantified by absorbance at 260 nm, and 5 μg of RNA were denatured in 6.5% formaldehyde and 50% formamide at 55 °C for 15 min. After addition of 20 × SSC (final concentration of 18.5 × SSC), the RNA was spotted at different concentrations (1 μg, 750 ng, and 500 ng) onto a nylon membrane (Hybond N, Amersham Buchler) using a manifold apparatus (Schleicher & Schuell, Dassel, Germany). Additional yeast tRNA (2, 1.5, and 1 μg; Boehringer Mannheim, Mannheim, Germany) was spotted in the same manner onto the nylon membrane. The nylon membrane was baked at 80 °C for 2 h and prehybridized in 5 × SSC for 10 min at 30 °C, followed by hybridization with ^{32}P-end-labeled oligo(dT)$_{12-18}$ (GibcoBRL, Eggenstein, Germany) at 30 °C overnight. The hybridization solution contained 5 × SSC, 50% (w/v) formamide, 0.5% (w/v) SDS, and 5 × Denhardt's solution (0.1% (w/v) Ficoll, 0.1% (w/v) polyvinylpyrrolidone, and 0.1% bovine serum albumin). Oligo(dT) (40 pmol) was 5′-end-labeled by incubation with 1 μl of 10 × forward exchange buffer (Promega, Heidelberg, Germany), 3 μl of [γ-^{32}P]ATP (10 mCi/ml), and 1 μl of T_4 polynucleotide kinase (8–10 units/μl; Promega) in nuclease-free water (total volume of 10 μl) for 10 min at 37 °C and cleaned up with the QIAquick™ nucleotide removal kit (QIAGEN, Hilden, Germany). The filter was washed four times in 2 × SSC for 5 min at room temperature and exposed to Kodak XAR-5 film at −70 °C. The hybridization signals were quantified densitometrically as described above. No signals were detected in the tRNA sample, demonstrating the specificity of the hybridization probe.

Expression of Cx30 in Xenopus Oocytes—For *in vitro* transcription of Cx30 mRNA, it was necessary to clone a DNA fragment that contained the complete coding region, but no upstream ATG triplets. The restriction map of the Cx30 gene revealed that such a fragment could not be derived by digestion with appropriate restriction enzymes. Therefore, we chose a polymerase chain reaction-based strategy. The Cx30 coding sequence was amplified using primers 5′-GAA TAA GCC TGC ACG ATG GAC-3′ and 5′-GCT CAC CTA CAC TTG ACC TTG-3′, which generated a 828-base pair fragment. This fragment was cloned in the *Sma*I site of the expression vector pBluescript SK$^+$ and completely sequenced on both strands. No *Taq* polymerase-induced nucleotide exchanges were detected in comparison with the original Cx30 phage insert DNA. The vector was linearized downstream of the Cx30 coding region by *Bam*HI digestion. After phenol/chloroform extraction, 10 μg were used as a template for *in vitro* transcription of 5′-capped cRNA using T7 RNA polymerase (Willecke *et al.*, 1991b). The cRNA was isolated according to the protocols and reagents in the RNaid kit (BIO 101, Inc. Vista, CA). Production of predominantly full-length transcripts was confirmed by electrophoresis in 1% agarose. The final concentration of Cx30 cRNA for injection was ~0.2 μg/μl.

Xenopus oocytes were stripped of the follicular membrane after a 1-h treatment with collagenase (2 mg/ml). Each oocyte was injected with 5 ng of an antisense oligonucleotide (5′-G CTT TAG TAA TTC CCA TCC TGC CAT GTT TC-3′) that is complementary to *Xenopus* Cx38 (commencing at nucleotide 5) alone or in combination with 8 ng (40 nl) of Cx30 cRNA. Similar amounts of cRNAs of Cx26 or Cx32, prepared as described above, from templates described by Barrio *et al.* (1991), were injected for analysis of the heterotypic channels. Oocytes were subsequently incubated in L-15 medium at room temperature for 1 day, after which the vitelline membranes were manually removed, and the oocytes were paired in various combinations (*i.e.* Cx30/oligonucleotide, Cx30/Cx30, Cx32/Cx30, and Cx30/Cx26). Functional expression was examined by a dual-cell voltage clamp.

For electrophysiological measurements, the two-electrode voltage-clamp method was used to clamp each oocyte (Harris *et al.*, 1981). The membrane potentials of the cells were measured, and the more negative one was used as the holding potential for both, typically −40 to −60 mV. Transjunctional voltage (V_j) was applied by clamping one cell at the holding potential and inducing different voltage steps of 1–30-s duration in the other cell. Records of both voltage and current in each cell provide direct measures of transjunctional voltage and current. Net conductance between oocytes was determined from the slope of the *I-V* relation.

The conductance at the initial moment of the voltage step (G_i) was obtained by fitting the decaying current to an exponential and extrapolating the current traces to $t = 0$. The steady-state conductance (G_{ss}; *i.e.* the conductance after the decaying current reached a steady-state level) was obtained as the offset term of the exponential fitting.

RESULTS

Cloning of the Mouse Cx30 Gene—Previously, we had screened a mouse genomic library of EMBL3 λ phages with rat Cx26 cDNA using low stringency hybridization conditions (Willecke *et al.*, 1991b). Here, we describe isolation of a recombinant phage clone that did not hybridize under stringent conditions to any of the known murine connexin genes. Restriction mapping and Southern blot hybridization revealed, within a 10.5-kb insert, two *Kpn*I fragments that cross-hybridized to Cx26 rat liver cDNA (Fig. 1). These fragments were subcloned and sequenced. They contained a complete connexin homologous open reading frame, as revealed by comparison with previously characterized connexin genes and cDNAs (Fig. 2). The ATG start codon was located in a consensus translation initiation context (Kozak, 1991). The open reading frame coded for a protein of 261 amino acids with a predicted molecular mass of 30,336 Da. We designated this new connexin as mouse Cx30 according to the nomenclature suggested by Beyer *et al.* (1987).

Analysis of Mouse Cx30 Amino Acid Sequence—The deduced amino acid sequence of mouse Cx30 shows the typical features of a connexin protein: it contains four potential transmembrane regions (the third of which exhibits a marked amphipathic character) and two putative extracellular loops with conserved cysteine residues, compared with other connexins (see Bennett *et al.* (1991)). The transmembrane domains (*underlined* in Fig. 2) were predicted by the algorithm of Rao and Argos (1986) and alignment to topological domains of rat Cx32 that were previously deduced from site-specific antibody studies (Milks *et al.*, 1988). Each of the two putative extracellular loops of mouse Cx30 contains three cysteine residues in the sequences CX_6CX_3C and CX_4CX_5C. Cx30 shows the highest overall amino acid identity to mouse Cx26 (77%), mouse Cx32 (57%), and

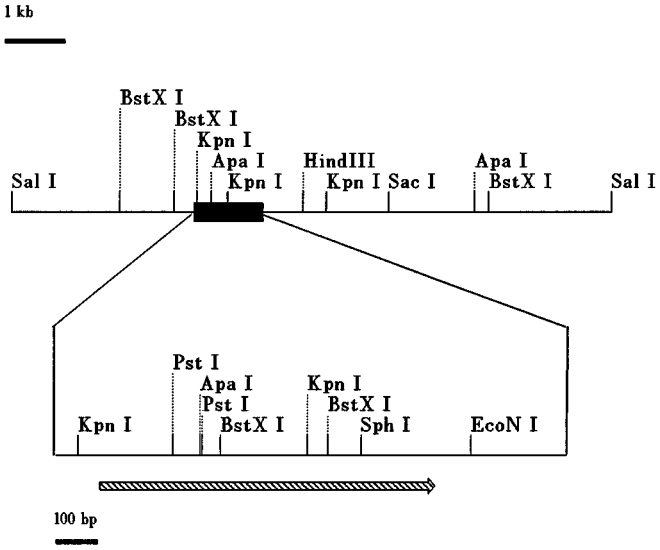

FIG. 1. **Map of the genomic clone containing the mouse Cx30 gene.** The *upper part* shows a restriction map of the 10.5-kb insert subcloned from a recombinant phage. Enlarged is a 1.2-kb fragment that contains the coding region of mouse Cx30. Its position and orientation are indicated by the *hatched arrow*. *bp*, base pairs.

Xenopus Cx30 (56%). Based on these comparisons, mouse Cx30 can be classified in the β-group of connexins (Gimlich *et al.*, 1990).

Table I shows the predicted pattern of amino acid identities among mouse Cx30, Cx26, and Cx43 (Hennemann *et al.*, 1992a, 1992d) and *Xenopus* Cx30 (Gimlich *et al.*, 1988) according to topological domains, as previously established for Cx32, Cx43, and Cx26 (Milks *et al.*, 1988; Yancey *et al.*, 1989; Zhang and Nicholson, 1994). It is evident that mouse Cx30 shows greater similarity to mouse Cx26 than to any other connexin protein sequence. Mouse Cx30 is probably not the rodent analogue of *Xenopus* Cx30, with which it shares only 56% amino acid identity. In particular, the cytoplasmic region C, which exhibits high divergence among connexins, shows 72% amino acid identity between mouse Cx30 and Cx26. For comparison, this domain shows only 11 and 29% sequence identities to mouse Cx43 and *Xenopus* Cx30, respectively. Fig. 3 illustrates the phylogenetic tree of all known murine connexin genes based on comparison of their amino acid sequences. It shows the close relationship and the relatively late divergence in evolution of Cx30 and Cx26 genes.

Genomic Organization and Chromosomal Localization—Comparison of connexin cDNAs with their respective genes has revealed a common feature of mammalian connexin genes: the complete coding region is located within a single exon. This coding exon is separated from the promoter by a large intron that can be between 3.8 kb (Cx26; Hennemann *et al.*, 1992d) and 8.5 kb long (Cx43; Yu *et al.*, 1994). The genomic organization of mouse Cx30 seems to comply with these criteria: the open reading frame is uninterrupted by introns. However, a possible splice acceptor site is located at positions −38 to −25 upstream of the start codon (Fig. 2), similar to the consensus sequence determined by Shapiro and Senapathy (1987). This is preceded by a possible lariat consensus motif at positions −53 to −59, suggesting the 3′-end of an intron.

Southern blot hybridization of a Cx30 probe to mouse genomic DNA, digested with different restriction enzymes, indicated that a single copy of the Cx30 gene exists in the mouse genome (Fig. 4*A*). Under these conditions, single DNA fragments of 9, 12, 5.8, and 9.5 kb were detected after digestion with *Bgl*II, *Eco*RI, *Nco*I, and *Sac*I. Fig. 4*B* illustrates the result

```
                                                -160      -150       -140       -130      -121
                                                cacatgaccttataatttcactatggtattggtcagataattc

          -110       -100       -90        -80        -70       -61
tgaggtaccttctactaattagcttggttctttttgtatgtttaagaataagcctgcacg

          -50        -40        -30        -20        -10        -1
cacatgaccttataatttcactatggtattggtcagATAATTCTGAGGTACCTTCTACTA

1         10         20         30         40         50         60
ATGGACTGGGGGACCCTGCACACCGTCATCGGTGGCGTGAACAAGCACTCTACCAGCATA
MetAspTrpGlyThrLeuHisThrValIleGlyGlyValAsnLysHisSerThrSerIle

          70         80         90         100        110        120
GGGAAGGTGTGGATCACGGTCATCTTTATTTTCCGAGTCATGATCCTAGTGGTGGCTGCC
GlyLysValTrpIleThrValIlePheIlePheArgValMetIleLeuValValAlaAla

          130        140        150        160        170        180
CAGGAAGTGTGGGGTGATGAGCAGGAGGACTTTGTCTGCAACACTCTGCAGCCAGGGTGC
GlnGluValTrpGlyAspGluGlnGluAspPheVal**Cys**AsnThrLeuGlnProGly**Cys**

          190        200        210        220        230        240
AAGAACGTCTGCTATGACCATTTCTTCCCGGTGTCTCACATCCGGCTCTGGGCCCTGCAG
LysAsnVal**Cys**TyrAspHisPhePheProValSerHisIleArgLeuTrpAlaLeuGln

          250        260        270        280        290        300
CTGATCTTTGTGTCTACCCCAGCCCTGTTGGTGGCCATGCACGTGGCCTACTACAGACAT
LeuIlePheValSerThrProAlaLeuLeuValAlaMetHisValAlaTyrTyrArgHis

          310        320        330        340        350        360
GAAACTGCCCGAAAGTTTATACGTGGGGAGAAGAGAAACGAGTTTAAAGACCTGGAGGAC
GluThrAlaArgLysPheIleArgGlyGluLysArgAsnGluPheLysAspLeuGluAsp

          370        380        390        400        410        420
ATCAAACGGCAGAAGGTGCGCATTGAGGGCTCCCTGTGGTGGACGTACACCAGCAGCATT
IleLysArgGlnLysValArgIleGluGlySerLeuTrpTrpThrTyrThrSerSerIle

          430        440        450        460        470        480
TTCTTCCGCATCATCTTCGAAGCCGCCTTCATGTATGTGTTCTACTTCCTCTACAATGGG
PhePheArgIleIlePheGluAlaAlaPheMetTyrValPheTyrPheLeuTyrAsnGly

          490        500        510        520        530        540
TACCACCTACCCTGGGTACTGAAATGTGGCATTGACCCCTGCCCCAATCTCGTGGACTGC
TyrHisLeuProTrpValLeuLys**Cys**GlyIleAspPro**Cys**ProAsnLeuValAsp**Cys**

          550        560        570        580        590        600
TTCATTTCGAGGCCAACTGAGAAAACGGTGTTCACTGTTTTTATGATTTCCGCATCCGTG
PheIleSerArgProThrGluLysThrValPheThrValPheMetIleSerAlaSerVal

          610        620        630        640        650        660
ATTTGCATGCTGCTCAATGTGGCCGAGTTGTGTTACCTGCTGCTTAAATTGTGCTTTAGG
IleCysMetLeuLeuAsnValAlaGluLeuCysTyrLeuLeuLeuLysLeuCysPheArg

          670        680        690        700        710        720
AGATCCAAAAGAACACAGGCGCAGAGAAACCACCCCAACCATGCCCTGAAAGAGAGCAAG
ArgSerLysArgThrGlnAlaGlnArgAsnHisProAsnHisAlaLeuLysGluSerLys

          730        740        750        760        770        780
CAGAATGAAATGAATGAGCTGATCTCAGATAGTGGCCAGAATGCAATCACAAGTTTCCCA
GlnAsnGluMetAsnGluLeuIleSerAspSerGlyGlnAsnAlaIleThrSerPhePro

          790        800        810        820        830        840
AGTTAAGCACTTCAAGGTCAAGTGTAGGTGAGCCCTTCTGAGCATGTACCCTCTTTGTAG
Ser
```

FIG. 2. **Genomic nucleotide and deduced amino acid sequences of mouse Cx30.** At the 5′-end, a putative splice acceptor site (positions −25 to −38) indicates a potential intron sequence (*lower-case letters*) in this region, similar to other characterized connexin genomic sequences (Fishman *et al.*, 1991; Willecke *et al.*, 1991a; Hennemann *et al.*, 1992a). Potential transmembrane regions according to the algorithm of Rao and Argos (1986) are *underlined*. Connexin-specific conserved cysteine residues in the extracellular domain are shown in *boldface letters*. The nucleotide sequence data are available from GenBank™/EMBL/DDBJ under accession no. 270023.

of Southern blot hybridizations with restriction enzyme-cleaved DNA from mouse × Chinese hamster hybrid cells that contained the different sets of mouse chromosomes listed in Table II. After hybridization of *Xba*I-digested DNA to the Cx30 genomic probe, a 12-kb fragment was obtained with mouse parental DNA, whereas a 1.3-kb fragment was seen with hamster parental DNA. Table II indicates that there is very strong correlation between the 12-kb band and the presence of mouse chromosome 14 in the corresponding hybrid cell lines. The only discordant EBS 2 hybrid cells harbored a fragment of mouse chromosome 14 that presumably did not contain the Cx30 gene. Thus, the gene for mouse Cx30 is assigned to chromosome 14. We suggest the genetic symbol *Gjb-6* as the designation for the

TABLE I

Amino acid identities of the putative topological domains of mouse Cx30 compared with those of mouse Cx26 and Cx43 and Xenopus Cx30

Number in parentheses represent percent amino acid similarity (*i.e.* residues of similar chemical properties).

Putative topology of mouse Cx30	Residues in mouse Cx30	Amino acid identities		
		To mouse Cx26	To mouse Cx43	To *Xenopus* Cx30
			%	
Cytoplasmic region A	1–21	81 (95)	38 (62)	57 (76)
Transmembrane region 1	22–41	75 (95)	50 (80)	55 (90)
Extracellular region B	42–74	91 (94)	66 (72)	73 (76)
Transmembrane region 2	75–94	95 (95)	60 (70)	95 (95)
Cytoplasmic region C	95–130	72 (86)	11 (17)	29 (49)
Transmembrane region 3	131–150	85 (95)	50 (60)	85 (95)
Extracellular region D	151–188	66 (79)	51 (70)	61 (76)
Transmembrane region 4	189–208	75 (90)	25 (70)	65 (90)
Cytoplasmic region E	209–261	56 (75)[a]	8 (11)	32 (45)

[a] For residues 209–224 (16 amino acids only). The Cx26 protein sequence is 35 residues shorter than the Cx30 sequence.

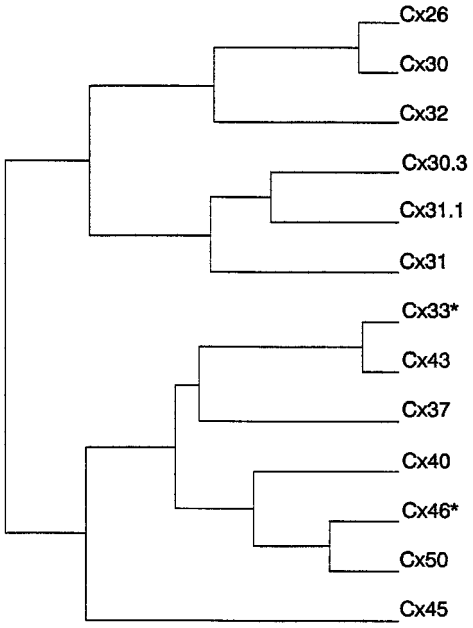

FIG. 3. **Phylogenetic tree of connexins.** The dendrogram was deduced by CLUSTAL analysis of total mouse protein sequences, except Cx33* and Cx46*, for which rat sequences were used since the corresponding mouse sequences have not been published.

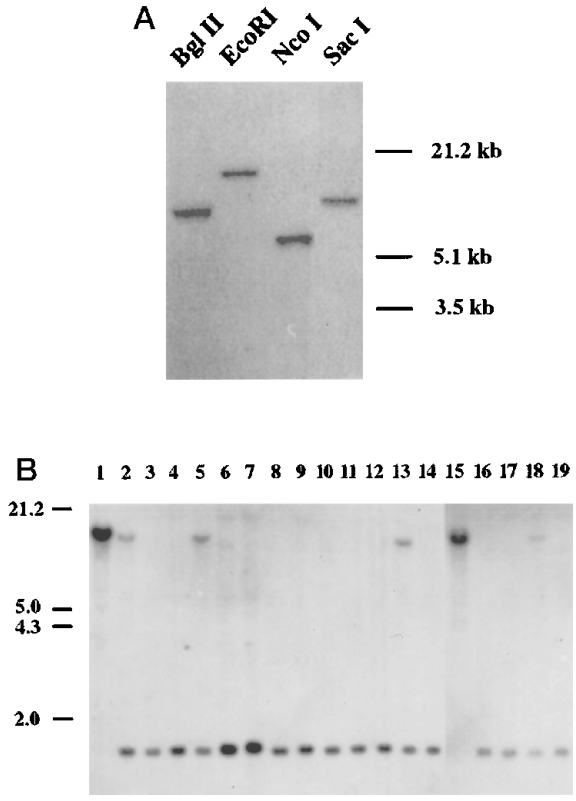

FIG. 4. **Mouse Cx30 is a single copy gene located on chromosome 14.** *A*, Southern blot hybridization of mouse DNA. A probe encompassing nucleotides 25–615 of Cx30 in Fig. 2 was hybridized to mouse genomic DNA digested with the restriction enzymes indicated. The single bands detected in each lane suggest that a single copy of the Cx30 gene exists in the haploid mouse genome. *B*, Southern blot hybridization of *Xba*I-digested DNA from mouse × Chinese hamster hybrid cell clones (*lanes 2–13* and *16–18*), mouse control cells (*lanes 1* and *15*), and hamster control cells (*lanes 14* and *19*). *Lanes 2–13* correspond to EBS 1 through EBS 15Az and *lanes 16–18* to EBS 51 through EBS 13Az, respectively, as listed in Table II. A mouse-specific hybridization fragment of 12 kb was detected only in DNA from cell hybrids EBS 1 (*lane 2*), EBS 5 (*lane 5*), EBS 15Az (*lane 13*), and EBS 13Az (*lane 18*), consistent with the presence of mouse chromosome 14 in these hybrid cells (see Table II).

mouse Cx30 gene, in extension of the nomenclature used for designation of known mouse connexin genes (*cf.* Schwarz *et al.* (1992, 1994)).

Expression of Cx30 mRNA—Total RNA from several mouse tissues was prepared (Chomczynski and Sacchi, 1987), electrophoretically separated, and hybridized under stringent conditions (50% formamide, 5 × SSC at 42 °C) to the mouse Cx30 gene probe described under "Materials and Methods." Preliminary experiments had shown that probe specificity and stringency of hybridization were sufficient to prevent cross-hybridization to Cx26 mRNA. Fig. 5*A* illustrates that expression of Cx30 mRNA is most abundant in adult brain and skin. Less abundant expression was detected in the uterus, lung, and eye tissue. Very low expression was seen in the testis and sciatic nerve. Cx30 mRNA was not detected in the liver, which exhibits abundant expression of the highly related Cx26 gene (Zhang and Nicholson, 1989). In all tissues that express Cx30 transcripts, two mRNAs species of 2.3 and 2.0 kb were detected, the latter one being much more abundant. Interestingly, the ratio of these two transcripts differed between mouse tissues. In adult brain and testis, the 2.3-kb Cx30 transcript contributed 35 and 50%, respectively, to the total amount of Cx30 mRNA as determined by quantitative densitometric evaluation of the double bands. In adult skin, uterus, and lung, the 2.0-kb mRNA was ~10-fold more abundant than the 2.3-kb transcript. We have normalized the relative amounts of Cx30 transcripts (signals of 2.0- and 2.3-kb mRNAs added) to the amount of poly(A)$^+$ mRNA in these tissues (see "Materials and Methods"). Normalized expression levels are indicated in Fig. 5*B*.

Furthermore, we have studied in more detail whether expression of Cx30 mRNA in the brain is developmentally regulated. Cx30 transcripts were not detected before birth. Weak expression was seen after 2 weeks of postnatal brain develop-

TABLE II

Segregation of mouse Cx30 genes and mouse chromosomes in mouse × Chinese hamster somatic cell hybrids

Southern hybridization analyses and chromosome determination of hybrid cells were performed on the same cell passage. A hybrid cell line was considered positive for a chromosome if >10% of the cells had one copy.

Cell hybrid	Mouse chromosome																			Mouse Cx30 gene
	1	2	3	4	5	6	7	8	9	10	11	12	13	14	15	16	17	18	19	X	
EBS 1	+	+	+	+	(+)[a]	+	+	+	+	+	−	+	+	+	+	+	+	+	+	+	+
EBS 2	+	+	+	−	−	+	+	+	+	+	−	+	+	(+)	+	+	+	−	+	+	−
EBS 4	−	−	−	−	−	−	−	−	−	−	−	−	+	−	+	−	+	−	−	(+)	−
EBS 5	+	+	+	+	−	+	+	+	−	+	−	+	+	+	+	+	+	+	+	+	+
EBS 9	−	+	−	−	−	+	+	+	+	−	−	+	+	−	+	−	+	+	+	(+)	−
EBS 11	−	−	−	−	−	−	+	−	−	+	−	+	−	−	+	+	−	−	−	+	−
EBS 13	+	+	+	+	−	+	+	+	+	+	−	+	+	−	+	+	+	+	+	+	−
EBS 15	−	+	+	+	−	+	+	+	−	+	−	+	+	−	+	+	+	−	+	+	−
EBS 17	+	+	−	−	−	−	+	−	+	−	−	−	+	−	+	−	+	−	−	+	−
EBS 5Az	+	+	+	−	−	+	+	+	−	−	−	+	+	−	+	+	+	+	+	−	−
EBS 9Az	−	+	+	+	−	−	+	+	−	+	−	+	+	−	+	+	+	+	+	−	−
EBS 15Az	+	+	+	+	−	+	+	+	+	−	−	+	+	+	+	+	+	+	+	−	+
EBS 51	−	+	+	−	+	+	+	+	+	−	−	+	−	−	+	+	+	+	+	+	−
EBS 58	+	+	+	+	−	+	+	−	+	+	−	+	+	−	+	−	+	−	−	+	−
EBS 13Az	−	+	−	−	−	−	+	−	−	+	−	+	−	+	+	+	+	−	+	−	+
Concordant hybrids	9	6	7	10	11	7	5	7	7	8	11	6	5	14	4	7	5	8	8	4	
Discordant hybrids	6	9	8	5	4	8	10	8	8	7	4	9	10	1	11	8	10	7	7	11	
Discordancy (%)	40	60	53	33	26	53	66	53	53	46	26	60	66	66	73	53	66	46	46	73	

[a] (+) indicates that a fragment of the chromosome was present.

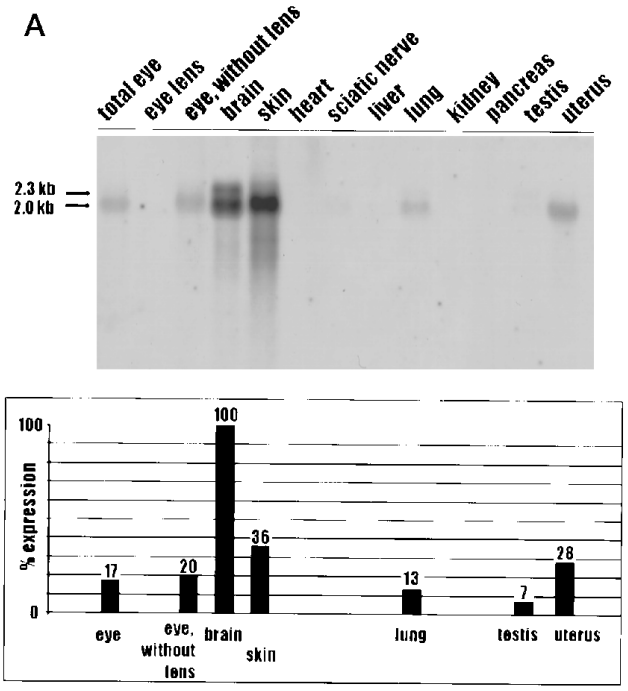

FIG. 5. **Tissue-specific expression of mouse Cx30 mRNA as detected by Northern blot hybridization and autoradiography.** *A*, total RNA (20 μg/lane) from adult mouse tissues was electrophoresed, blotted, and probed with a genomic mouse Cx30 probe (as described under "Materials and Methods"). Two transcripts of 2.0 and 2.3 kb were detected, being most abundant in the brain, skin, and uterus. *B*, expression of Cx30 mRNAs was standardized against abundance of poly(A)$^+$ RNA in each tissue sample using [^{3}H]oligo(dT) (see "Materials and Methods"). The amount of Cx30 transcripts in the brain was set equal to 100%. Note that autoradiographic intensities of both Cx30 mRNA transcripts were added for this comparison.

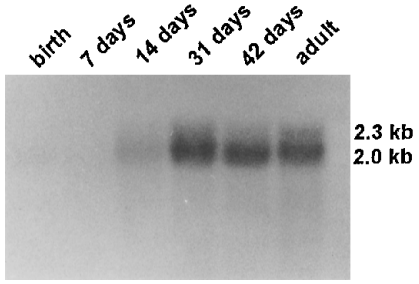

FIG. 6. **Developmental expression of Cx30 mRNA in mouse brain.** Samples of total RNA (20 μg/lane) were isolated from mouse brain at the developmental stages indicated and subjected to Northern blot hybridization as described in the legend to Fig. 5. Significant amounts of Cx30 mRNA were detected 2 weeks after birth and became most abundant in adult brain.

ment (Fig. 6). When the amounts of Cx30 mRNA in mouse brain were standardized by hybridization to a cytochrome cDNA probe (Hennemann *et al.*, 1992b), it became obvious that the brain at 4 and 6 weeks and in adult mice contained similar amounts of Cx30 transcripts (Fig. 6).

Functional Expression of Mouse Cx30 in Xenopus Oocytes—Capped Cx30 RNA was synthesized *in vitro* using T7 RNA polymerase and injected into stage VI *Xenopus* oocytes. Following incubation overnight at 19 °C, oocytes were stripped of their vitelline envelopes and paired for a further 16–20 h before recording intercellular conductance with two-electrode voltage clamps. For this experimental series, these conditions yielded coupled oocytes from injections of control cRNA for Cx32 at ~50% of the time. This frequency was lower than usual as the toads were entering their "nonproductive" season. The background of endogenous coupling was eliminated as described previously by injection of an antisense oligonucleotide to bases −5 to 25 of *Xenopus* Cx38 (numbering from the initiation codon for translation) (Ebihara *et al.*, 1989).

Cx30 formed functional homotypic channels in *Xenopus* oocytes (13 out of 25 pairs) with conductances ranging from 0.5 to 3 microsiemens. Quantitative analysis of junctional currents induced by Cx30 showed that initial junctional conductance (G_i) decreased with increasing positive or negative V_j (Fig. 7). G_i showed an asymmetry, with a slight decline in response to hyperpolarizing voltages and a larger decline with depolarizing voltages. Part or all of this decline in G_i at higher V_j may result from systematic errors introduced from extrapolation to $t = 0$ of the exponential fits to the current decays as the time constants become markedly shorter with increasing V_j (Fig. 7*A*). In fact, the dependence of the time constant of the current decay on V_j was the steepest we have yet recorded of any connexin. The voltage gating responses of G_{ss} of Cx30 channels, obtained from depolarizing and hyperpolarizing pulses, are described by slightly different Boltzmann relationships, with parameters of $A = 0.13$, $V_o = +37.7$ mV, and $G_{min} = 0.25$ for depolarizing

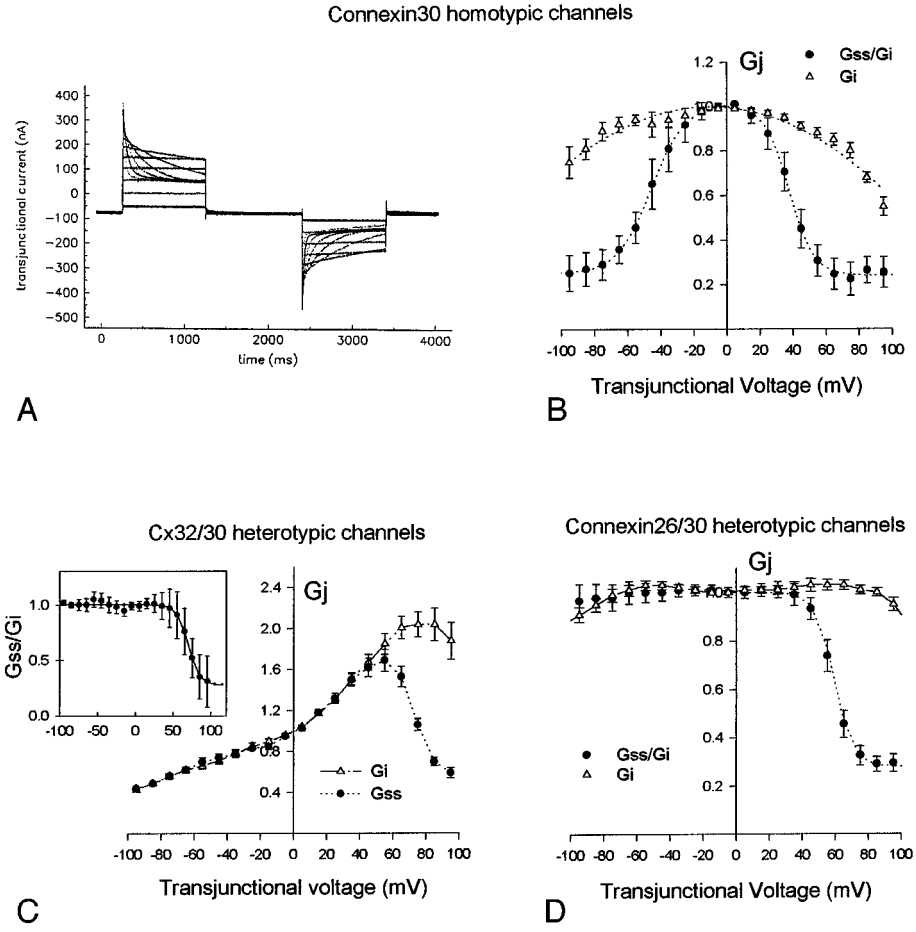

FIG. 7. **Electrical coupling of Cx30.** *A*, recordings of transjunctional current through Cx30 gap junctions expressed in oocytes. Voltage pulses of 1-s duration, ranging from 5 to 105 mV and from −5 to −105 mV, in 10-mV increments were applied to one cell, while the other was clamped at its resting potential of −60 mV. Note the marked increase in the rate of current decay with increasing voltage. Values of G_i and G_{ss} were obtained by extrapolations of exponential fits of the current decay to $t = 0$ and $t =$ infinity, respectively. *B*, plots of G_i (normalized to the values obtained at + or −5 mV) or steady-state conductance (G_{ss}/G_i, G_{ss} normalized to G_i at the same V_j) *versus* V_j. G_i showed asymmetric declines at higher voltages that are likely to be due, at least in part, to the limited time resolution of the system as channel kinetics became faster with increasing V_j. Normalized G_{ss} values from depolarizing (positive V_j) or hyperpolarizing (negative V_j) voltage pulses were fit by distinct Boltzmann relations with the following parameters: $A = 0.13$, $V_o = 37.7$ mV, and $G_{min} = 0.25$ for positive V_j and $A = 0.10$, $V_o = 45.7$ mV, and $G_{min} = 0.26$ for negative V_j. *C*, plots of G_i and G_{ss} *versus* V_j for Cx32/Cx30 heterotypic pairings, with the Cx30 cell defined as the positive pole. Both G_i and G_{ss} were normalized to conductance at 0 mV (interpolated between + and −5 mV). Rectification of G_i and the unilateral gating response of G_{ss} were similar to those observed in Cx32/Cx26 heterotypic combinations, with steeper instantaneous rectification (slope of G_i *versus* $V_j = 0.010$ mV^{-1}). The drop in G_i at larger positive V_j was presumably analogous to that described for the homotypic channels in *B*. The unilateral gating response of V_j can be obtained by fitting G_{ss}/G_i *versus* V_j to a Boltzmann relation with the parameters $A = 0.136$, $V_o = 69.8$ mV, and $G_{min} = 0.28$ (*inset*). *D*, plots of G_i and G_{ss}/G_i (normalized as described for *B*) *versus* V_j for Cx26/Cx30 heterotypic pairings. Positive V_j was defined as depolarizing pulses in the Cx30-expressing oocyte or as hyperpolarizing pulses in the Cx26-expressing oocyte. Gating characteristics at positive V_j were similar to those of Cx30 homotypic channels, although a Boltzmann fit to the data yielded slightly different parameters ($A = 0.18$, $V_o = 59.2$ mV, and $G_{min} = 0.28$). A similar increase in the V_o of the Cx26 hemichannel would move its voltage response beyond the recorded range.

pulses and $A = 0.10$, $V_o = -45.7$ mV, and $G_{min} = 0.26$ for hyperpolarizing pulses. Paired *t* tests of the G_{ss} values for equivalent hyper- and depolarizing V_j pulses demonstrated this asymmetry to be significant at the 0.05 to 0.02 probability level. The asymmetry in G_{ss} is independent of that seen in G_i as we plot the G_{ss}/G_i ratio in Fig. 7. The asymmetric responses of both G_i and G_{ss} to V_j are consistent with a sensitivity to transmembrane or inside-outside voltage (V_{i-o}). However, preliminary studies utilizing different holding potentials for both oocytes ranging from $V_m = 120$ to 0 mV revealed no obvious sensitivity of conductance to V_{i-o}, although it remains possible that the relatively minor asymmetries seen in Fig. 7, if arising to V_{i-o}, may require more extensive statistical analysis to detect.

Cx30 also formed functional heterotypic channels with Cx32 (7 out of 13 pairs) and Cx26 (7 out of 12 pairs) in *Xenopus* oocytes, with junctional conductances ranging from 1 to 5 microsiemens and from 1 to 8 microsiemens, respectively. The Cx32/Cx30 pairing produced highly rectifying channels that showed only a slow voltage gating response when the Cx30 side was made relatively positive (Fig. 7*C*). Boltzmann parameters describing this response were obtained from replotting of G_{ss}/G_i *versus* V_j (see Fig. 7*C*, *inset*) and fitting, with values of $A = 0.136$, $V_o = 69.8$ mV, and $G_{min} = 0.28$. This behavior was analogous to that reported for Cx32/Cx26 pairs. Rapid rectification, also characteristic of Cx32/Cx26 heterotypic junctions, was evident in the G_i plot of the Cx32/Cx30 response to V_j. The increase in conductance with positive V_j (defined with respect to the Cx26- or Cx30-expressing oocyte) was even steeper with Cx30 (0.009 mV^{-1}) than with Cx26 (0.0055 mV^{-1}) (Barrio *et al.*, 1991).

Cx30/Cx26 pairings did not show significant rectification of G_i other than that likely to be attributable to an extrapolation error of the rapidly decaying currents at large positive V_j. The G_{ss} plot showed an asymmetry that was somewhat predictable from the respective homotypic behaviors of Cx30 and Cx26

(Fig. 7*D*). The heterotypic interaction appeared to cause an increase in the V_o of each of the hemichannel responses compared with the homotypic case, such that no significant gating of the Cx26 hemichannel was evident within the range tested.

DISCUSSION

The new mouse Cx30 gene is closely related to the mouse Cx26 gene, with which it shares 77% sequence identity, more than with any other connexin gene described so far. We have assigned the Cx30 gene to mouse chromosome 14, which also contains the genes for Cx26 and Cx46 (Schwarz *et al.*, 1992). Thus, presumably the Cx30 and Cx26 genes arose by gene duplication. The dendrogram of all murine connexin genes (Fig. 3) supports the notion of a common origin of these genes, late in evolution relative to other connexin genes. Whereas the cytoplasmic loop of the mouse β-connexin proteins Cx26 and Cx32 shows only 37% sequence identity (*cf.* Fig. 4*B* of Hennemann *et al.* (1992c), for example), the Cx26 and Cx30 proteins exhibit 72% identity in this region.

Several findings support our conclusion that mouse Cx30 is a functional connexin gene. First, the genomic Cx30 sequence has all the features characteristic of other functional rodent connexin genes, *i.e.* the reading frame is uninterrupted by introns, but there is a possible intron upstream of the initiation site for translation. Second, the Cx30 amino acid sequence deduced from the nucleotide sequence contains four potential transmembrane regions characteristic of connexins. The extracellular cysteine residues found in all connexin proteins and potentially involved in recognition and docking of hemichannels (John and Revel, 1991; Dahl *et al.*, 1992) are conserved as well. Third, the coding region of Cx30 hybridizes to two specific transcripts of 2.3 and 2.0 kb in several mouse tissues. Fourth, when Cx30 cRNA is expressed in *Xenopus* oocytes, it forms gap junction channels exhibiting unique voltage dependence.

The different sizes of the mouse Cx30 mRNA could be due to different start points of transcription, alternative splicing, or different lengths of the 3′-untranslated region. Alternative splicing has recently been detected in the rodent Cx32 gene. Schwann cells express Cx32 mRNA using an alternative promoter located in the large intron upstream of the coding exon (Neuhaus *et al.*, 1995; Söhl *et al.*, 1996). In addition, a third Cx32 transcript is expressed in embryonic stem cells.[2] Two additional mouse connexin genes, Cx30.3 and Cx31, exhibit transcripts of two different sizes (reviewed by Willecke *et al.* (1991a)). Since a large intron is conserved in the 5′-untranslated region of all connexin genes, one can speculate that alternative promoter usage may be a common feature for regulation of connexin gene expression.

Upon expression of the cRNA of Cx30 in the *Xenopus* oocyte system, robust currents between cell pairs were recorded. Surprisingly, the voltage sensitivity of these currents was slightly asymmetric, showing greater decrements in both G_j and G_{ss} with depolarizing voltage pulses (see Fig. 7, *A* and *B*). The kinetics of the current decay showed a strong dependence on V_j for both polarities. Given the poor temporal resolution of the oocyte system (clamping times are typically 10 ms), this posed a problem for obtaining accurate estimates of G_j at high voltages. Despite efforts to extrapolate the exponential decays to zero, some apparent decreases in G_j were seen. While this is likely to be due to extrapolation errors, we cannot discount the possibility that this reflects a real V_j-activated gate with kinetics that are not resolved by our clamps.

The steady-state conductance of these channels showed asymmetrical gating in response to V_j, even when G_{ss} values were normalized to G_i for each value of V_j. This was most evident in Boltzmann fits of the data that yielded different parameters for hyperpolarizing and depolarizing voltage pulses, most notably with respect to V_o (−45 and 37 mV, respectively). This asymmetry could arise from sensitivity of the channels to transmembrane voltage differences, although this would have to be of the opposite polarity to that seen for the closest homologue studied to date, Cx26. However, no overt dependence of transjunctional conductance on the original holding potential of the cell (from −120 to 0 mV) was observed. An alternative possibility could be an asymmetric contribution of heterotypic channels between Cx30 and *Xenopus* Cx38, although this seems unlikely as no conductance was ever seen to develop between Cx30 and endogenous *Xenopus* Cx38. Finally, it is formally possible that the docking process between connexins could differentially affect the voltage gates in the two hemichannels. Such a phenomenon has not been seen to date and seems unlikely given the reported mirror image symmetry of the two halves of a gap junction.

Another surprising result is the lack of similarity in the gating profiles in response to V_j for Cx30 and its close homologue, Cx26. Cx30 channels responded at significantly lower voltages (V_o = 37–45 mV) than Cx26 (V_o = 89 mV) and also showed faster kinetics of closure by at least an order of magnitude (see Fig. 7*A*). Noticeably, the time constant of decay is more strongly dependent on V_j than that of any other connexin we have studied in oocytes.

Other general characteristics of Cx30, revealed in heterotypic pairings with Cx26 or Cx32, were more similar to the properties of Cx26. Heterotypic pairings with Cx26 showed asymmetrical voltage gating (Fig. 7*D*), consistent with each hemichannel gating with positive voltage at its cytoplasmic face, but with V_o increased over that seen in homotypic channels (*cf.* V_o = 59 mV with V_o = 37–45 mV for Cx30 homotypic channels and $V_o > 105$ mV with V_o = 89 mV for Cx26 homotypic channels). Such increases in V_o may reflect increases in the activation energy required for channel closure, a property that may be influenced by the nature of the docking interaction between hemichannels.

Cx32/Cx30 heterotypic channels showed even greater rectification characteristics than reported for Cx32/Cx26 (Fig. 7*C*) (*cf.* Barrio *et al.* (1991)). Based on previous analyses of Cx32/Cx26 channels (Verselis *et al.*, 1994), the asymmetric G_{ss} response of Cx32/Cx30 channels to V_j further supports the conclusion that Cx30 channels gate when their cytoplasmic ends are relatively positive. The rapid rectification seen in the G_i *versus* V_j plot of Cx32/Cx26 has recently been demonstrated not to represent gating, but to reflect the properties of each channel that change conductance with voltage (Bukauskas *et al.*, 1995).[3] It is largely explained by significant differences in the relative selectivity of the two channels for cations and anions (Cx32, slightly anionically selective; Cx26, cationically selective).[3] By this criterion, Cx30 and Cx26 would be expected to share similar ionic selectivity, although the steeper rectification of G_i seen in Cx32/Cx30 channels (0.010 mV^{-1}) compared with Cx32/Cx26 channels (0.005 mV^{-1}) might suggest that Cx30 channels are even more strongly cationically selective than Cx26 channels.

The expression pattern of mouse Cx30 transcripts was different from that of Cx26 mRNA. For example, no expression of Cx30 was found in the liver and pancreas, which expressed relatively high levels of Cx26 (Zhang and Nicholson, 1989). Both genes were expressed in the brain, skin, and uterus. The

[2] E. Dahl, H. Hennemann, G. Hallas, U. Dahl, and K. Willecke, submitted for publication.

[3] T. M. Suchyna, M. Chilton, J. M. Nitsche, R. D. Veenstra, and B. J. Nicholson, submitted for publication.

quantitative comparison of Cx30 mRNA expressed in different tissues (Fig. 5) showed that expression was most abundant after 4 weeks of postnatal development in the brain. This was clearly different from Cx26, which is more highly expressed in prenatal brain and decreases after birth (Dermietzel *et al.*, 1989). Cx30 gap junction channels appear to be characteristic of adult mouse brain.

The expression of both Cx30 and Cx32 (the latter associated with oligodendrocytes and some neurons; see Dermietzel and Spray (1993)) raises the interesting possibility of formation of rectifying channels such as those reported above in the oocyte system. In a tissue showing the rapid local fluctuations in voltage seen in the central nervous system, such channels could play a significant role in preferentially directing impulse propagation. A critical future goal will be to use *in situ* hybridization and peptide-specific antibodies to resolve the expression pattern of mouse Cx30 at the cellular level. This will reveal whether Cx30 is expressed in neurons or glial cells. Electrophysiological experiments, reviewed by Dermietzel and Spray (1993), have indicated that the CA3 region of rat hippocampus contains gap junctions that do not react with antibodies to Cx43, Cx32, or Cx26 proteins. Cx30 is an interesting candidate for analysis of unidentified gap junction proteins and channels in the brain. Furthermore, since there are relatively few amino acid differences between Cx26 and Cx30 proteins, it is possible that some of the described antibodies, directed to Cx26-derived peptides or the total Cx26 protein, may cross-react with the Cx30 protein. Thus, the specificity of Cx26 antibodies has to be reanalyzed and carefully compared with that of Cx30 antibodies. These experiments are currently underway in our laboratory. Both the similarities and differences in the channel properties of Cx30 and Cx26, given their high level of sequence identity, raise exciting prospects for identification of specific domains, or even residues, that influence characteristics such as voltage, gating kinetics, and permeability.

Acknowledgment—We thank Gaby Hallas for expert technical assistance.

REFERENCES

Barrio, L. C., Suchyna, T., Bargiello, T., Xu, L. X., Roginski, R., Bennett, M. V. L., and Nicholson, B. J. (1991) *Proc. Natl. Sci. U. S. A.* **88,** 8410–8414
Bennett, M. V. L., Barrio, L. C., Bargiello, T. A., Spray, D. C., Hertzberg, E., and Saez, J. C. (1991) *Neuron* **6,** 305–320
Beyer, E. C. (1993) *Int. Rev. Cytol.* **173c,** 1–37
Beyer, E. C., Paul, D. L., and Goodenough, D. A. (1987) *J. Cell Biol.* **105,** 2621–2629
Bruzzone, R., Haefliger, J. A., Gimlich, R. L., and Paul, D. L. (1993) *Mol. Biol. Cell* **4,** 7–20
Bukauskas, F. F., Elfgang, C., Willecke, K., and Weingart, R. (1995) *Pfluegers Arch. Eur. J. Physiol.* **429,** 870–872
Chomczynski, P., and Sacchi, N. (1987) *Anal. Biochem.* **162,** 156–159
Dahl, G., Werner, R., Levine, E., and Rabadan-Diehl, C. (1992) *Biophys. J.* **62,** 172–180
Dermietzel, R., and Spray, D. C. (1993) *Trends Neurosci.* **16,** 186–192
Dermietzel, R., Traub, O., Hwang, T. K., Beyer, E., Bennett, M. V. L., Spray, D. C., and Willecke, K. (1989) *Proc. Natl. Acad. Sci. U. S. A.* **86,** 10148–10152
Ebihara, L., Beyer, E. C., Swenson, K. I., Paul, D. L., and Goodenough, D. A. (1989) *Science* **243,** 1194–1195
Elfgang, C., Eckert, R., Lichtenberg-Fraté, H., Butterweck, A., Traub, O., Klein, R. A., Hülser, D. F., and Willecke, K. (1995) *J. Cell Biol.* **129,** 805–817
Fishman, G. I., Moreno, A. P., Spray, D. C., and Leinwand, L. A. (1991) *Genomics* **10,** 250–256
Gimlich, R. L., Kumar, N. M., and Gilula, N. B. (1988) *J. Cell Biol.* **107,** 1065–1073
Gimlich, R. L., Kumar, N. M., and Gilula, N. B. (1990) *J. Cell Biol.* **110,** 597–605
Haefliger, J.-A., Bruzzone, R., Jenkins, N. A., Gilbert, D. J., Copeland, N. G., and Paul, D. L. (1992) *J. Biol. Chem.* **267,** 2057–2064
Harley, C. B. (1987) *Gene Anal. Tech.* **4,** 17–22
Harris, A. L., Spray, D. C., and Bennett, M. V. L. (1981) *J. Gen. Physiol.* **77,** 95–117
Hennemann, H., Suchyna, T., Lichtenberg-Fraté, H., Jungbluth, S., Dahl, E., Schwarz, H.-J., Nicholson, B. J., and Willecke, K. (1992a) *J. Cell Biol.* **117,** 1299–1310
Hennemann, H., Schwarz, H.-J., and Willecke, K. (1992b) *Eur. J. Cell Biol.* **57,** 51–58
Hennemann, H., Dahl, E., White, J. B., Schwarz, H.-J., Lalley, P. A., Chang, S., Nicholson, B. J., and Willecke, K. (1992c) *J. Biol. Chem.* **267,** 17225–17233
Hennemann, H., Kozjek, G., Dahl, E., Nicholson, B. J., and Willecke, K. (1992d) *Eur. J. Cell Biol.* **58,** 81–89
John, S. A., and Revel, J.-P. (1991) *Biochem. Biophys. Res. Commun.* **178,** 1312–1318
Kozak, M. (1989) *J. Cell Biol.* **108,** 229–241
Milks, L. C., Kumar, N. M., Houghten, R., Unwin, N., and Gilula, N. B. (1988) *EMBO J.* **7,** 2967–2975
Moreno, A. P., Rook, M. B., Fishman, G. I., and Spray, D. C. (1994) *Biophys. J.* **67,** 113–119
Neuhaus, I. M., Dahl, G., and Werner, R. (1995) *Gene* (*Amst.*) **158,** 257–262
Paul, D. L. (1986) *J. Cell Biol.* **103,** 123–134
Paul, D. L. (1995) *Curr. Opin. Cell Biol.* **7,** 665–672
Rao, J. K. M., and Argos, P. (1986) *Biochim. Biophys. Acta* **869,** 197–214
Sambrook, J., Fritsch, E. F., and Maniatis, T. (1989) *Molecular Cloning: A Laboratory Manual*, 2nd Ed., Cold Spring Harbor Laboratory, Cold Spring Harbor, NY
Schwarz, H.-J., Chang, Y. S., Hennemann, H., Dahl, E., Lalley, P. A., and Willecke, K. (1992) *Somat. Cell Mol. Genet.* **18,** 351–359
Schwarz, H.-J., Chang, Y. S., Lalley, P. A., and Willecke, K. (1994) *Somat. Cell Mol. Gen.* **20,** 243–247
Shapiro, M. B., and Senapathy, P. (1987) *Nucleic Acids Res.* **15,** 7155–7175
Söhl, G., Gillen, C., Gleichmann, M., Müller, H. W., and Willecke, K. (1996) *Eur. J. Cell Biol.* **69,** 267–275
Tabor, S., and Richardson, C. C. (1987) *Proc. Natl. Acad. Sci. U. S. A.* **84,** 4767–4771
Verselis, V. K., Ginter, G. S., and Bargiello, T. A. (1994) *Nature* **368,** 348–351
White, T. W., Bruzzone, R., Goodenough, D. A., and Paul, D. L. (1992) *Mol. Biol. Cell* **3,** 711–720
White, T. W., Bruzzone, R., and Paul, D. (1995) *Kidney Int.* **48,** 1148–1157
Willecke, K., Hennemann, H., Dahl, E., Jungbluth, S., and Heynkes, R. (1991a) *Eur. J. Cell Biol.* **56,** 1–7
Willecke, K., Heynkes, R., Dahl, E., Stutenkemper, R., Hennemann, H., Jungbluth, S., Suchyna, T., and Nicholson, B. J. (1991b) *J. Cell Biol.* **114,** 1049–1057
Yancey, S. B., John, S. A., Lal, R., Austin, B. J., and Revel, J.-P. (1989) *J. Cell Biol.* **108,** 2241–2254
Yu, W., Dahl, G., and Werner, R. (1994) *Proc. R. Soc. Lond. B Biol. Sci.* **255,** 125–132
Zhang, J.-T., and Nicholson, B. J. (1989) *J. Cell Biol.* **109,** 3391–3401
Zhang, J.-T., and Nicholson, B. J. (1994) *J. Membr. Biol.* **139,** 15–29

Molecular Cloning and Functional Expression of Mouse Connexin-30,a Gap Junction Gene Highly Expressed in Adult Brain and Skin

Edgar Dahl, Dieter Manthey, Ye Chen, Hans-Jürgen Schwarz, Young Sook Chang, Peter A. Lalley, Bruce J. Nicholson and Klaus Willecke

J. Biol. Chem. 1996, 271:17903-17910.
doi: 10.1074/jbc.271.30.17903